EFFECTS OF DAYLIGHTING ON THE ANNUAL HEATING AND COOLING ENERGY USE IN OFFICE BUILDINGS

Wonuk Kim[1], Jongug Jeon[2], Honghee Park[1], Jooseong Lee[1] and Yongchan Kim[1]

[1] Department of Mechanical Engineering, Korea University, Seoul, Korea

[2] Department of Architecture, Korea University, Seoul, Korea

1. Abstract

Daylightable floor area can be determined by the geometries such as window area, perimeter area, and floor area. The daylightable floor area ratio (DFR), which is defined as the ratio of the daylightable floor area to the total floor area, decreases with an increase in the floor area. In this study, the heating and cooling energy consumption of office buildings was simulated by using eQUEST(DOE-2.2). The energy performance of the buildings applying dimming control of lighting with daylight was estimated by varying the floor area (six cases) and window-to-wall ratio (WWR) (four cases). The relationships for the reduction in the annual heating and cooling energy according to daylight and DFR in office buildings were developed by using a multiple regression analysis. As a result, the annual cooling energy in the buildings decreased, but the annual heating energy increased by applying daylight as lighting. The reduction rate in the annual cooling energy of the buildings with large floor area was smaller than that of the buildings with small floor area. The buildings having high WWR showed smaller energy reduction rate due to an increase in infiltration and thermal heat transfer through window. The increasing rate in the annual heating energy of the buildings with large floor area was larger than that of the buildings with small floor area. The buildings having high WWR showed smaller increasing rate of the annual heating energy due to an increase in radiation heat transfer through window.

2. Introduction

The global warming due to the use of fossil fuel has been accelerated rapidly. The Korean government has been made a lot of efforts to reduce the emission of carbon dioxide. In Seoul city, approximately 40% of the energy was used in the building sector (Bang, 2009). The retrofit of the energy facilities or redesign of the buildings has been considered to reduce the energy consumption in the building sector. In general commercial buildings, 40% of the total energy consumption in the buildings was used for HVAC systems and 20~30% was used for artificial lighting (EIA, 2005). Electric lighting is the largest single-end energy use in office buildings. Several methods to reduce artificial lighting energy, such as efficient ballasts, dimming control of lighting devices, have been tried. These methods showed higher net present value and internal return rate than HVAC facilities (Doukas et al., 2009), so the lighting retrofit was preferred to other options.

One of the efficient methods to save lighting energy in the buildings is to adopt daylight. Krarti et al. (2005) developed a simplified method to calculate artificial lighting energy reduction with different window transmittances and areas. Designers who have an interest on daylighting as an energy saving method can use their equations to easily calculate the lighting energy reductions by use of daylighting when the window type and window-to-wall ratio (WWR), and building geometries are known. Lighting using daylight makes secondary effects on the heating and cooling energy consumption due to the change of artificial lighting and radiation. Li et al. (2005) conducted an analysis for the effect of daylighting on the peak cooling load in a generic office building located in Hong Kong using DOE-2.1E. Three single glazing types of clear, tinted, and reflective glasses were considered. Two independent variables, daylighting aperture (DA) and the overall thermal transfer value (OTTV), were adopted. The OTTV is an indication of the average heat gain through the building envelope. They developed a correlation for the incremental peak electricity use (IPEU) according to OTTV and DA. However, they assumed constant infiltration of 0.6 air change per hour which could not respond the change of infiltration upon various WWR. Sezgen and Koomey (2000) studied the impact of lighting loads upon building heating and cooling energy consumption for eleven different building types of “new” and “existing” vintages in five distinct climates. Lighting heat dissipation had approximately no net impact upon HVAC primary energy consumption.

The daylightable area can be determined by the parameters such as the WWR, the ratio of the window area to the perimeter area and the ratio of the perimeter area to the floor area. As the gross area of the building increases, DFR decreases, which leads to a decrease in the effects of daylight on the energy consumption of the building (Morofsky, 2001). It is required to know the daylightable area and lighting and HVAC loads according to light dimming control with daylighting for proper system design in a given building geometry. However, a simple correlation to calculate building loads with various geometries is very limited in the open literature. The objectives of this study are to analyze the effect of light dimming control with daylight on the annual heating and cooling load by building simulation and to develop a simplified correlation for prediction of the annual heating and cooling load considering light dimming control with daylight. The effects of lighting dimming control with daylight on the annual heating and cooling load in the buildings were analyzed by varying the floor area, WWR, and window materials using DOE-2.2E. In addition, based on the simulation results, two correlations for incremental annual heating and cooling energy consumptions were developed by using regression analysis. The crack method was used for the estimation of infiltration.

3. Model descriptions

3.1. Building models

Fig. 1 shows the air view of the modeled building, which is a typical rectangle ten-story (including three-underground-stories) office building. Six building models, whose total floor area varies from 5,000 m^2 to 30,000 m^2, were selected for the analysis. The office buildings have the same perimeter zone depth of 4.6 m from exterior wall (ASHRAE, 2007). As the total floor area of the buildings increases, the ratio of the total perimeter area to the total floor area decreases. Typical densities and schedules for office buildings were used to model occupancy, lighting, and equipment (Table 1). A window set consists of an aluminum spacer, 6 mm double clear glass, and 13 mm air-space. The window set has the conductivity of 8.35 W/ m^{2o}C.

When solar light is excessive to use, a shading device is essential in case of using daylight for lighting. In the simulation, external windows of the building have shading schedule. When the space is occupied, 20 percent of blind is closed. Otherwise, 80 percent of blind is closed.

In this study, a recessed fluorescent model was used which does not vent in the return or supply air. The lighting power density was set to 10.76 W/m^2 in according to standard office value (ASHRAE, 2007). In the perimeter zone, dimming control of artificial lighting was used to reduce lighting energy by daylighting. It was assumed that the dimmable lighting device consumes 36% of the rated power when it has 20% of the rated light intensity.

Daylighting was modeled in the perimeter zone of the building. Typical external windows can effectively daylight the perimeter zone to a depth of 2 times of the head height of the window (ISENA, 2000) as shown in Fig. 2. The daylightable depth for 10% WWR was about 80% of the perimeter zone depth and the entire area of the perimeter zone was daylightable for 30% WWR.

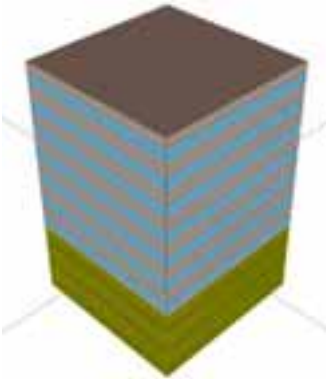

Fig. 1: Air view of the office building (7500 m^2, WWR 20%)

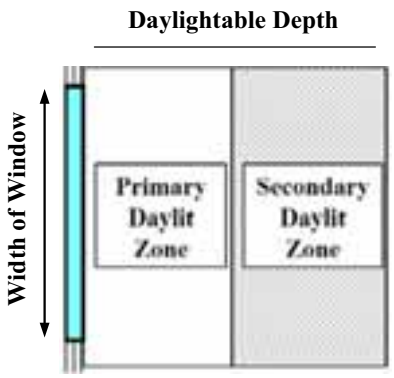

Fig. 2: Schematic diagram of daylightable depth

Table 1 Brief descriptions of the office building

Section		Details
Location		Incheon (latitude 37.6N, longitude 127.0E)
Building type and stories		Office building, 7 above grade, 3 below grade
Total floor area		5,000 ~30,000 m^2
Dimensions and heights		1x1 ratio (rectangle), floor-to-floor 3.65 m
Operating hours		Mon. to Fri. : 08-18
HVAC design parameter		Lighting load=10.76 W/ m^2; Equipment load=10.76 W/ m^2
		Space design temperature : Cooling=26°C, Heating=22°C
Construction of building envelope	External walls	6.4 mm glass + 19 mm insulation board + 13 mm gypsum board (U-value=0.48 W/ m^2 °C)
	Roof	10 mm roof build-up + 76 mm polyurethane + 16 mm plywood (0.24 W/ m^2 °C)
	Windows	6 mm double clear glass + 13 mm air-space (8.35W/ m^2 °C)

In DOE-2.2E, hourly measured horizontal solar radiation from the weather data are used for calculating interior illuminance and glare index. First, the program calculates daylight factors based on building construction material and environment. In the next step, exterior horizontal illuminance from the measured horizontal solar radiation is multiplied with the stored daylight factors. Eventually, the interior illuminance and glare index are calculated.

In DOE-2.2E daylighting model, maximum two reference points are allowed and the fraction of lighting area at each reference point can be set. Artificial lights in the daylightable area of the perimeter zone should be controlled according to the illuminance at the reference points. Two references were set at 25% and 75% of the daylightable zone depth, respectively, and their height was 76.2 cm from the floor. A continuous lighting dimming control was selected with the maximum 500 lx.

Infiltration is affected by WWR. However, most of the infiltration models could not represent the change in infiltration flow with window area. DOE-2.2E includes five infiltration methods which are crack, air-change, Sherman-Grimsrud, ASHRAE-enhanced, and residential. Among them, only the crack method can represent the change of the infiltration flow according to window area. In the crack method, there are two infiltration flow equations for exterior wall of Eq. (1) and window of Eq. (2), respectively.

$$\text{Infiltration flow of exterior wall(cfm)} = k_{wall} \cdot dP^{0.8} \cdot A_{wall} \quad (1)$$

$$\text{Infiltration flow of window(cfm)} = k_{win} \cdot dP^{0.5} \cdot P_{win} \quad (2)$$

In the Korean Standard (KS, 2003), the high air-tight window should have the infiltration flow less than 0.56 L/s/m^2 at 10 Pa, providing the coefficient for window, k_{win}, 2.0, in the crack method. Field et al. (2010) used 2.03 L/s/m^2 for the infiltration flow per exterior wall area at a pressure difference of 75 Pa between inside and outside of the wall in their simulation study. The infiltration coefficient of exterior wall was calculated using the value suggested by Field et al. (2010), which yielded the coefficient for exterior wall, k_{wall}, of 0.4.

To conduct load and energy simulation of the building in Inchon city, Korea, we used the weather data from Energy Efficiency and Renewable Energy (EERE) of U.S. Department of Energy (DOE) which is the International Weather for Energy Calculation (IWEC) type.

3.2. Parametric analysis

A parametric analysis was carried out for 72 different cases which consist of six floor areas, three glaze types, and four WWRs. Table 2 summarizes the cases used in the analysis. The height and width of the fenestration

were determined by WWR of the buildings. The WWR of the buildings was varied from 10% to 40%. Three different glazing types with various U-factor, SHGC and visible transmittance were modeled with different geometries of the building. Table 3 lists the glazing types used in the analysis.

Table 2 Window size and number with WWR and floor area

A_f	WWR	No. of Window	Window height(m)	Window width(m)
500	0.1	11	0.95	0.85
	0.2		1.16	1.38
	0.3		1.38	1.75
	0.4		1.59	2.02
750	0.1	13	0.95	0.82
	0.2		1.16	1.33
	0.3		1.38	1.69
	0.4		1.59	1.95
1000	0.1	16	0.95	0.82
	0.2		1.16	1.35
	0.3		1.38	1.71
	0.4		1.59	1.97
1500	0.1	19	0.95	0.85
	0.2		1.16	1.39
	0.3		1.38	1.76
	0.4		1.59	2.03
2000	0.1	22	0.95	0.85
	0.2		1.16	1.38
	0.3		1.38	1.75
	0.4		1.59	2.02
3000	0.1	27	0.95	0.85
	0.2		1.16	1.38
	0.3		1.38	1.75
	0.4		1.59	2.02

Table 3 Window properties

Glazing	U-factor	SHGC	Visible trans
Glaze 1(Double clear)	0.64	0.7	0.78
Glaze 2(Double blue)	0.64	0.49	0.5
Glaze 3(Double Low-E)	0.5	0.67	0.721

4. Results of parametric analysis

4.1. Annual cooling and heating load

Fig. 3 shows the variation of the annual cooling and heating load with A_f for glaze 1. The annual cooling and heating load increased with an increase in the floor area. However, the increasing slope in the cooling load was significantly higher than that in the heating load. In addition, the cooling and heating load increased with an increase in WWR. These trends were also observed for glaze 2 and 3. The building load was influenced by the properties of a glaze. As shown in Fig. 4, the building with glaze 1 and glaze 3 showed higher annual

cooling load than the building with glaze 2 because of higher SHGC values. On the contrary, the building with both the highest U-factor and lowest SHGC showed the highest heating load.

As given in Eq. (3), the external heat gain includes the followings: conduction from wall and window, radiation through window, and convection heat transfer through infiltration and ventilation. The internal heat gain includes person, light, and equipment. Four parameters were selected as dominant values in the present analysis, which are A_f, A_{win}, SHGC·A_{win} and U-factor·A_{win}. A multiple regression analysis was conducted to develop a simple correlation based on the simulation results. Table 4 shows the coefficients of Eqs. (3-1) and (3-2). The predictions by the present correlation were consistent with the data from the simulations using DOE-2.2 with R^2 of about 1.

$$\begin{aligned}\text{Cooling / Heating Load} &= q_{\text{outside, heat gain}} + q_{\text{inside, heat gain}} \\ &= [q_{\text{cond, wall}} + q_{\text{cond, win}} + q_{\text{rad, sol}} + q_{\text{conv, inf}} + q_{\text{conv, vent}}] \\ &\quad +[q_{\text{person to space}} + q_{\text{light to space}} + q_{\text{equip to space}}] \\ &= [q_{\text{cond, wall}} + U_{win} \cdot A_{win} \cdot \Delta T + (E_D + E_d + E_r) \cdot SHGC \cdot A_{win} \\ &\quad +C \cdot (k_{win} \cdot dP^{0.5} \cdot P_{win} + k_{wall} \cdot dP^{0.8} \cdot P_{wall}) \cdot \Delta T + q_{\text{conv, vent}}] \\ &\quad +[q_{\text{person}} \cdot OD \cdot A_f + LPD \cdot A_f + EPD \cdot A_f]\end{aligned} \tag{3}$$

$$\text{Cooling Load} = a \cdot A_f + b \cdot A_{win} + c \cdot SHGC \cdot A_{win} + d \cdot U_{win} \cdot A_{win} + e \tag{3-1}$$

$$\text{Heating Load} = a \cdot \ln(A_f) + b \cdot A_{win} + c \cdot SHGC \cdot A_{win} + d \cdot U_{win} \cdot A_{win} + e \tag{3-2}$$

Table 4 Coefficients for the correlations for the annual cooling and heating load

Load	Coefficient of the correlation					R^2
	a	b	c	d	E	
Cooling	0.28823	0.13074	0.71681	-0.34039	-12.0803	0.99994
Heating	-35.214	0.1707	0.71729	-1.53844	120.3229	0.99469

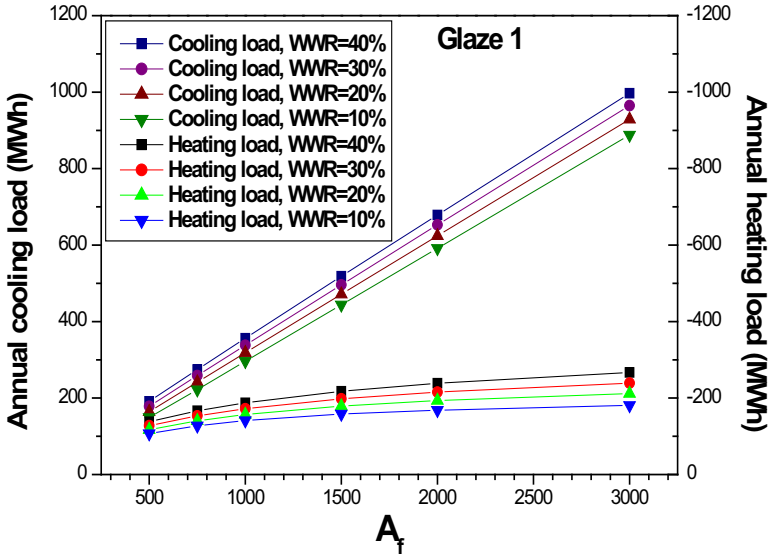

Fig. 3 Variation of annual cooling and heating load with A_f and WWR for glaze 1

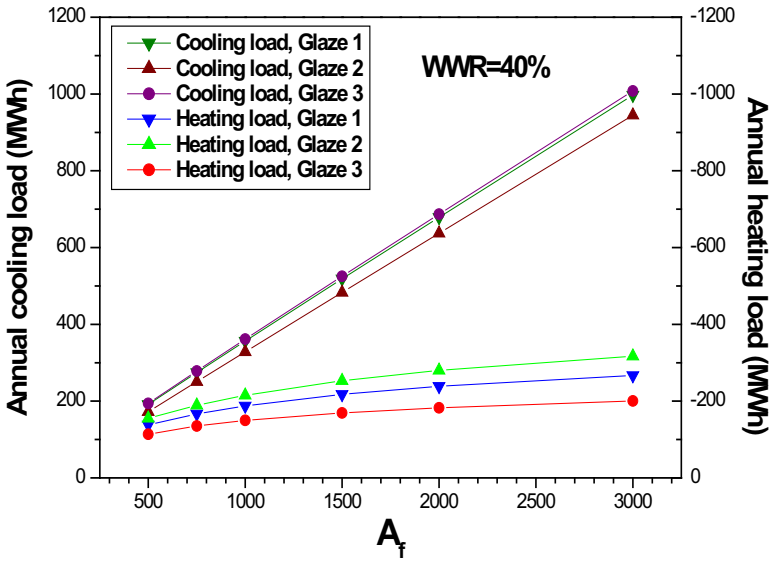

Fig. 4 Variation of annual cooling and heating load with A_f and glaze type for WWR=40%

4.2. Increment of the annual heating and cooling load by daylighting

The adoption of lighting dimming control with daylight to the building makes an effect on the cooling and heating load. Lighting load of the perimeter space decreases with the application of daylighting. The internal heat gain also varies due to less lighting load, resulting in a change of the HVAC load for the space. In addition, the external heat gain through the external wall and window will be changed simultaneously with the variation in the thermal properties of the space.

The ratio of the daylightable area to the floor area (DFR) was introduced to explain the effects of daylighting (CEC, 2008).

$$\mathrm{DFR} = \frac{(\text{Width of Window} + 1.22\text{m}) \times \mathrm{N}}{\text{Width of Floor}} \times \frac{\text{Daylightable Depth}}{\text{Perimeter Depth}} \times \frac{A_p}{A_f} \tag{4}$$

As shown in Fig. 5, the DFR varies as a function of the floor area and WWR. As the WWR of the building increases, the DFR also increases. However, the DFR becomes almost the same as the ratio of the perimeter area to the floor area when the WWR increases beyond 30%. The DFR decreases with an increase in the floor area of the building.

As shown in Eq. (5), the increase in the load was represented by the change of infiltration, solar heat gain and conduction through window, the change of internal heat gain from lighting, and the change of solar heat gain absorbed on floor. The internal lighting heat gain was estimated by the equation of Krarti et al. (2005). They introduced annual average daylight flux per unit floor area. However, in this study, daylight flux per unit daylightable floor area was used because the dimming control was performed based on the daylightable area. Eq. (5) was simplified as Eq. (5-1) in terms of dominant parameters, which are A_{win}, $SHGC \cdot A_{win}$, $U\text{-factor} \cdot A_{win}$, $T_v \cdot A_{win}/DFR$ and $DFR \cdot A_f$. The coefficients of the present correlation were determined by the multiple regression analysis. Table 5 shows the regression coefficients of Eq. (5-1). The predictions were consistent with the data from the simulations using DOE-2.2 with R^2 of 0.99 for cooling and 0.91 for heating.

$$\begin{aligned}\text{Incremental Load} = {} & a' \cdot k_{win} \cdot dP^{0.5} \cdot P_{win} \cdot \Delta T + b' \cdot (E_D + E_d + E_r) \cdot SHGC \cdot A_{win} \\ & + c' \cdot U_{win} \cdot A_{win} \cdot \Delta T + d' \cdot LPD \cdot \left(\frac{E_{v,out}}{E_{set}} \cdot \frac{T_v \cdot A_{win}}{DFR \cdot A_{floor}}\right) \cdot A_f \\ & + e' \cdot q_{solar\,absorbed} \cdot DFR \cdot A_f + f'\end{aligned} \tag{5}$$

$$\begin{aligned}\text{Incremental Load} \cong {} & a_{IL} \cdot A_{win} + b_{IL} \cdot SHGC \cdot A_{win} + c_{IL} \cdot U_{win} \cdot A_{win} + d_{IL} \cdot \frac{T_v \cdot A_{win}}{DFR} \\ & + e_{IL} \cdot DFR \cdot A_f + f_{IL}\end{aligned} \tag{5-1}$$

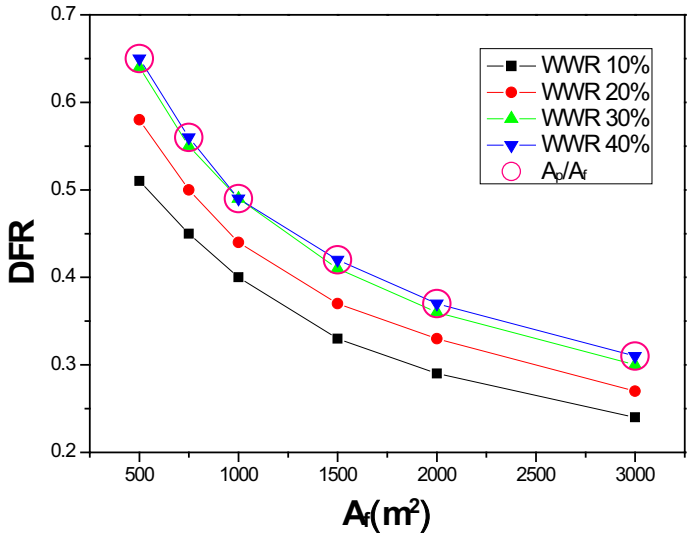

Fig. 5: DFR with floor area

Table 5 Coefficients for the correlations for the incremental cooling and heating load by daylighting

Increment of load	Coefficients of the correlation						R^2
	a_{IL}	b_{IL}	c_{IL}	d_{IL}	e_{IL}	f_{IL}	
Cooling	-0.01444	0.00118	-0.00711	-0.00201	0.03086	-0.8845	0.99147
Heating	-0.03789	-0.01448	0.06299	-0.00679	0.02048	1.80636	0.91166

4.3. Percent annual heating and cooling energy saving by daylighting

Figs. 6 and 7 show the variation of PCS_D and PHS_D with DFR. PCS_D and PHS_D indicate annual cooling and heating energy savings in percent, respectively, with the adoption of daylighting. As DFR increased from 0.25 to 0.55, PCS_D increased from approximately 2% to 4.5%. In addition, PHS_D increased from -7% to -3.5% with the increase in DFR from 0.25 to 0.6. In the building with the same WWR, the building having higher DFR showed more reduction in the cooling load and less increase in the heating load than the building having lower DFR, when the light dimming control with daylight used in the building. In addition, as shown in Fig. 7, glaze 3 showed more aggregation in PHS_D than other glazes because glaze 3 had the lowest U-factor. Therefore, the building with glaze 3 showed the lowest PHS_D among them.

As shown in Fig. 8, PCS_D decreased with an increase in WWR, while PHS_D increased with an increase in WWR. However, the case for 10% WWR in PHS_D was exceptional. This may be because glaze 2 transmits smaller daylight than the others, which leads to increase electric lighting to satisfy the reference illuminance of 500 lx. The building with glaze 2 showed the lowest annual cooling load due to smaller visual transmittance of glaze 2, but it showed the highest annual heating load due to bigger u-factor and smaller SHGC of glaze 2. Visual transmittance of glaze shows an influence on PCS_D, while U-factor of glaze makes an influence on PHS_D. Therefore, PCS_D and PHS_D are a function of A_{win}, A_f, glaze visual transmittance, glaze U-factor, and DFR.

PCS_D and PHS_D were estimated by the ratio of Eq. (4-1) to (5-1) and the ratio of Eq. (4-2) to (5-1), respectively. Figs. 9 and 10 show the deviations of the predicted PCS_D and PHS_D using the present correlation from the data using DOE-2.2, respectively. The present correlations for PCS_D and PHS_D showed quite satisfactory predictions with R^2 of 0.98 and 0.82, respectively.

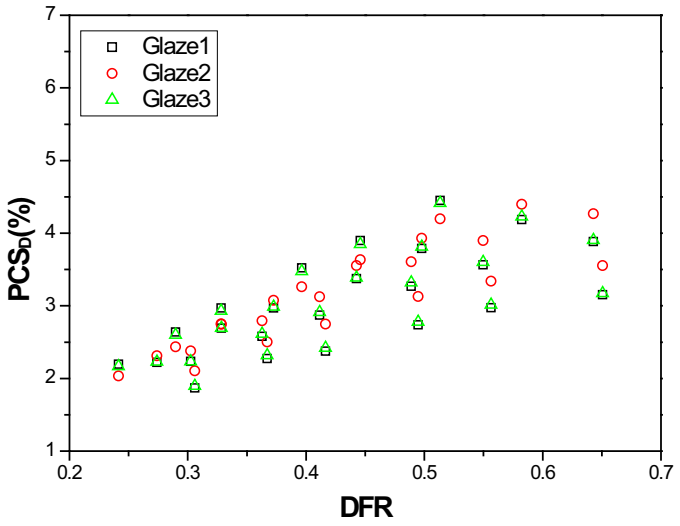

Fig. 6 Cooling load savings with DFR

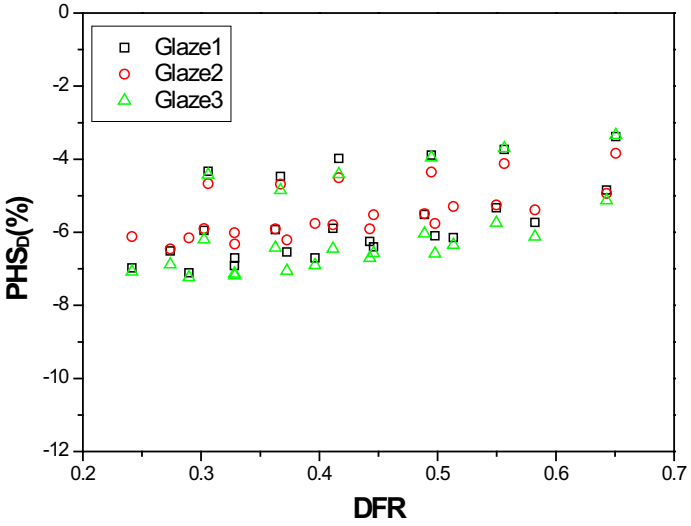

Fig. 7 Heating load savings with DFR

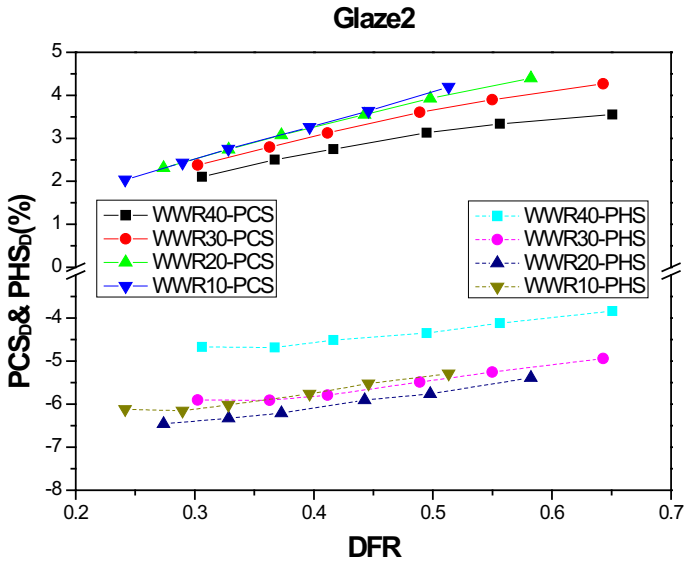

Fig. 8 Heating and cooling energy savings (%) with DFR for glaze 2

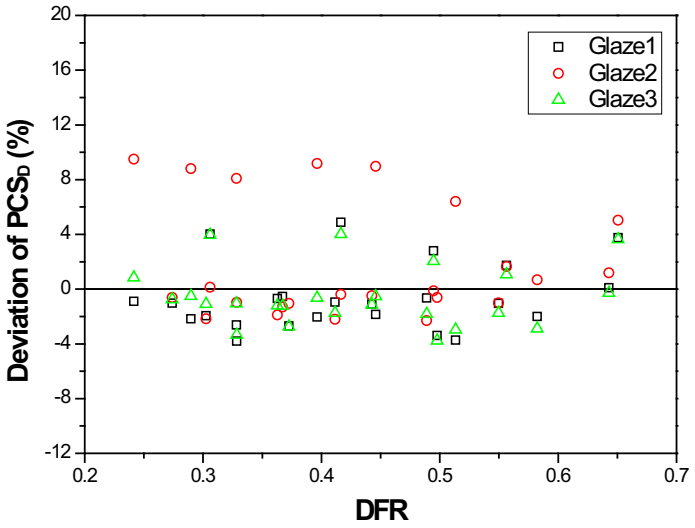

Fig. 9 Deviation of PCS_D with DFR

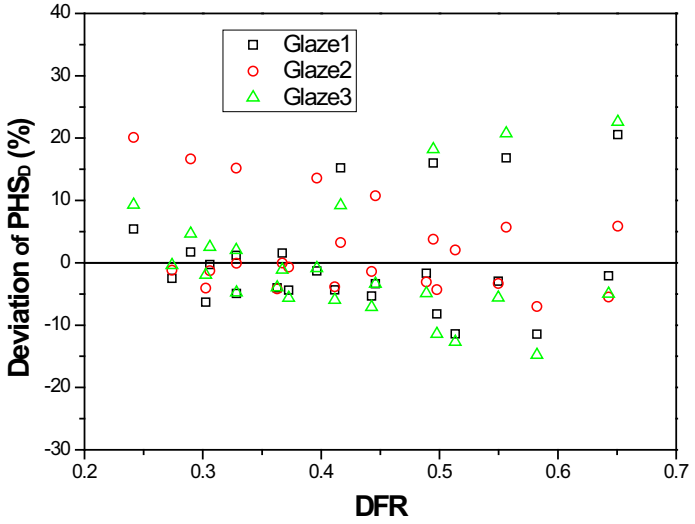

Fig. 10 Deviation of PHS_D with DFR

5. Conclusions

The effects of the building geometry, window area, window type by using lighting dimming control with daylight on the annual cooling and heating load savings were studied. The effects of lighting control with daylight on the cooling and heating load were affected by the window type and DFR. A correlation for the annual cooling and heating load of the building was developed as a function of DFR and total floor area. When the lighting dimming control with daylight is applied in the building, PCS_D and PHS_D decreased with an increase in the total floor area. The adoption of daylighting may decrease approximately 3% of the annual cooling load, but it may increase approximately 5.6% of the annual heating load. Eventually, daylighting had approximately no net impact on the annual heating and cooling load. However, it showed still meaning results for sizing HVAC facilities in the building. Moreover, lighting dimming control with daylight showed significant savings of artificial lighting load.

6. Acknowledgements

This research was supported by Seoul R&BD Program (ST090845).

7. References

ASHRAE, 2007. ANSI/ASHRAE/IESNA Standard 90.1-2007. American Society of Heating, Refrigerating, and Air Conditioning Engineers, Atlanta.

Bang, K.Y., 2009. Yearbook of regional energy statistics. Korea Energy Economics Institute.

CEC, 2008. 2008 Building Energy Efficiency Standards for Residential and Nonresidential Buildings, Technical Report CEC-400-2008-001-CMF. California Energy Commission, Sacramento.

Doukas, H., Nychtis, C., Psarras, J., 2009. Assessing energy-saving measures in buildings through an intelligent decision support model. Building and Environment 44(2), 290-298.

EIA., 2005. Commercial Buildings Energy Consumption Survey: Consumption and Expenditures Tables. http://www.eia.doe.gov/emeu/cbecs/ Washington, DC: U.S. Department of Energy, Energy Information Agency.

Field, K., Deru, M., Studer, D., 2010. Using DOE Commercial Reference Buildings for Simulation Studies. 4th national conference IPBPSA-USA.

IESNA, 2000. The IESNA Lighting Handbook: Reference and Application. Illuminating Engineering Society of North America, New York.

Korean Standard, 2003. KS-F 2292-88: The method of air tightness for windows and doors. Korean Standard, Korea.

Krarti, M., Erickson, P.M., Hillman, T.C., 2005. A simplified method to estimate energy savings of artificial lighting use from daylighting. Building and Environment 40, 747–754.

Li, D.H.W., Lam, J.C., Wong, S.L., 2005. Daylighting and its effects on peak load determination. Energy 30, 1817-1831.

Morofsky, E., 2001. Development of generic office building energy measures, Final Report. Caneta Research Inc., Canada.

Sezgen, O., Koomey, J.G., 2000. Interactions between lighting and space conditioning energy use in US commercial buildings. Energy 25, 793-805.